Space Weather®

RESEARCH ARTICLE
10.1029/2022SW003193

Space Weather Environment During the SpaceX Starlink Satellite Loss in February 2022

Tzu-Wei Fang[1], Adam Kubaryk[1,2], David Goldstein[3], Zhuxiao Li[1,2], Tim Fuller-Rowell[1,2], George Millward[1,2], Howard J. Singer[1], Robert Steenburgh[1], Solomon Westerman[3], and Erik Babcock[3]

[1]NOAA Space Weather Prediction Center, Boulder, CO, USA, [2]CIRES, University of Colorado Boulder, Boulder, CO, USA, [3]SpaceX Starlink, Hawthorne, CA, USA

Key Points:

- Geomagnetic storms lead to thermosphere expansion and increase satellite drag
- National Oceanic and Atmospheric Administration's coupled Whole Atmosphere Model and Ionosphere Plasmasphere Electrodynamics, a physics-based model, captures the enhanced neutral density environment responsible for the Starlink satellite loss event
- Alerts and warnings based on neutral density predictions during geomagnetic storms are critical for satellite drag estimation

Correspondence to:
T.-W. Fang,
tzu-wei.fang@noaa.gov

Citation:
Fang, T.-W., Kubaryk, A., Goldstein, D., Li, Z., Fuller-Rowell, T., Millward, G., et al. (2022). Space weather environment during the SpaceX Starlink satellite loss in February 2022. *Space Weather*, *20*, e2022SW003193. https://doi.org/10.1029/2022SW003193

Received 14 JUN 2022
Accepted 24 OCT 2022

Author Contributions:
Conceptualization: Tzu-Wei Fang, Howard J. Singer
Data curation: David Goldstein, Zhuxiao Li, Solomon Westerman, Erik Babcock
Formal analysis: Adam Kubaryk
Investigation: Tzu-Wei Fang, Solomon Westerman
Methodology: Tzu-Wei Fang
Resources: Robert Steenburgh, Solomon Westerman, Erik Babcock
Software: Adam Kubaryk, Zhuxiao Li
Visualization: Adam Kubaryk, George Millward
Writing – original draft: Tzu-Wei Fang, George Millward

Abstract On 3 February 2022, SpaceX Starlink launched and subsequently lost 38 of 49 satellites due to enhanced neutral density associated with a geomagnetic storm. This study examines the space weather conditions related to the satellite loss, based on observations, forecasts, and numerical simulations from the National Oceanic and Atmospheric Administration Space Weather Prediction Center (SWPC). Working closely with the Starlink team, the thermospheric densities along the satellite orbits were estimated and the neutral density increase leading to the satellite loss was investigated. Simulation results suggest that during the geomagnetic storm, pre-launch Monte Carlo analyses performed by the Starlink team using empirical neutral density inputs from NRLMSISE-00 tended to underestimate the impact relative to predictions from the operational coupled Whole Atmosphere Model and Ionosphere Plasmasphere Electrodynamics physics-based model. The numerical simulation indicated this minor to moderate geomagnetic storm was sufficient to create 50%–125% density enhancement at altitudes ranging between 200 and 400 km. With the increasing solar activity of Solar Cycle 25, satellites in low-Earth orbit are expected to experience an increasing number of thermospheric expansion events. Currently, no alerts and warnings issued by SWPC are focused on satellite users concerned with atmospheric drag and related applications. Thus, during geomagnetic storms, it is crucial to establish suitable alerts and warnings based on neutral density predictions to provide users guidance for preventing satellite losses due to drag and to aid in collision avoidance calculations.

Plain Language Summary SpaceX Starlink lost 38 of 49 satellites after the launch of Group 4-7 in February 2022 due to enhanced neutral density associated with a geomagnetic storm. Based on observations, forecasts, and numerical simulations from the National Oceanic and Atmospheric Administration Space Weather Prediction Center (SWPC), this study provides a detailed analysis of the space weather conditions and neutral density environment during the event. Simulation results suggest that during this minor to moderate geomagnetic storm, the neutral density enhancement was about 50%–125% increase at altitudes ranging between 200 and 400 km. The operational coupled Whole Atmosphere Model and Ionosphere Plasmasphere Electrodynamics physics-based model demonstrates better performance compared to empirical thermospheric neutral density models, one of which was used by the Starlink team. With an increasing number of satellites in low-Earth orbit, it becomes crucial for SWPC to establish suitable alerts and warnings based on neutral density predictions to provide users guidance for preventing satellite losses due to drag and to aid in collision avoidance calculations.

1. Space Weather Event and Space-X Starlink Launch

Upper atmosphere expansion can lead to changes in thermospheric density that affect satellite drag in low-Earth orbit (LEO, <2,000 km), and more specifically in this case under consideration, in very low Earth orbit (VLEO, 250–450 km). The primary density effect arises from an increase in temperature resulting from energy input to the thermosphere driven by solar or geomagnetic activity, which causes the atmosphere to expand and increase neutral density at a fixed altitude in Earth's upper atmosphere. The neutral density response depends on neutral composition and varies as a function of altitude and solar cycle. It has been well established that changes in neutral density directly affect the drag on LEO/VLEO satellites and may become more critical with emerging commercial initiatives to establish large constellations of small satellites and CubeSats. A good characterization of the range of neutral density variation and accurate forecasts of these events ahead of the arrival of solar and

Writing – review & editing: David Goldstein, George Millward, Howard J. Singer, Robert Steenburgh

geomagnetic storms can potentially benefit satellite operations and are crucial for both orbital prediction/tracking and collision avoidance.

Commencing on 29 January 2022, a series of Coronal Mass Ejection (CME) erupted on the Sun, propagated toward Earth, and were subsequently observed by the Solar and Heliospheric Observatory (SOHO) spacecraft at the L1 point (1st Lagrange point), which is about 1% of the distance from the Earth toward the Sun. The CME propagation was also captured by the concurrent off-axis images from STEREO A spacecraft. The solar wind plasma traveled from the Sun with an elevated speed of around 500 km per second toward the Earth. With the estimated solar wind speed and simulations from numerical models, forecasters at the Space Weather Forecast Office (SWFO) in the National Oceanic and Atmospheric Administration (NOAA) Space Weather Prediction Center (SWPC) predicted that the fast speed solar wind would hit Earth within 3–4 days. A few days later, on 3 February, the CMEs arrived at Earth with the strong southward interplanetary magnetic field (IMF Bz) producing a geomagnetic storm in the near-Earth environment, including perturbations in the thermosphere and ionosphere. Based on various observations in space and on the ground, shown in Figure 1, the CME event enhanced the global geomagnetic activity Kp index (a 3-hr index based on measurements from ground-based magnetometers around the world) to a value of 5, and the enhancement lasted for 6 hours on both 3 and 4 February (see the red bars in the bottom panel of Figure 1). The Kp values indicated that the event was classified as a minor storm according to SWPC's Space Weather Scales (https://www.swpc.noaa.gov/noaa-scales-explanation). The observed IMF Bz at L1 reached −19 on the 3 February and −10 nT on 4 February together with a solar wind speed of more than 500 km/s on both days. The 2-day event would be expected to lead to significant impacts on the thermosphere and ionosphere based on previous studies (e.g., Bruinsma et al., 2021; T. J. Fuller-Rowell et al., 2021; Huang et al., 2016; Qian et al., 2019).

Shortly after the space weather event, on 8 February, SpaceX issued a press release (https://www.spacex.com/updates/) describing the loss of 38 Starlink satellites on 4 February apparently due to enhanced neutral density associated with the space weather event. On 3 February SpaceX launched 49 Starlink v1.5 satellites (Group 4-7) to slightly eccentric orbits with 350 km apogee, 210 km perigee, and 53° inclination. The targeted final altitude for this set of satellites was 550 km. The maneuver and thrusting for orbit raising typically occurs within 2 days of the launch date. As reported by SpaceX, this set of satellites experienced an increase in neutral atmospheric drag relative to previous launches, which was not anticipated. The Starlink team was only able to command 11 of the 49 satellites to a safehold attitude to effectively "take cover from the storm." The remaining 38 satellites could not overcome the increased drag and reentered the Earth's atmosphere just days after the launch. NOAA-SWPC worked closely with the Starlink team to analyze the neutral atmosphere environment for the event to describe the neutral density changes associated with the minor but prolonged geomagnetic storm. The neutral densities estimation in this study are largely based on the SWPC's operational coupled Whole Atmosphere Model and Ionosphere Plasmasphere Electrodynamics model (WAM-IPE). Satellite orbits and onboard observations were provided by the Starlink team within SpaceX for direct comparison with operational model predictions.

Since 2009 through February 2022, there have been more than 40 SpaceX launches that were dedicated to deploy the Starlink system. Figure 2 illustrates the 2-day integrated 3-hr Kp index (launch day and the day after) and daily F10.7 (solar radio flux at 10.7 cm, 2,800 MHz) from prior launches with satellite perigees below 275 km. Several launches occurred after the event in February 2022, but most of the launches targeted insertion altitudes above 300 km until June 2022. Both geomagnetic activity and solar fluxes can impact thermospheric density. F10.7 is an indicator commonly used for thermospheric density variations on time scales of a solar rotation (28 days), several months, and over the 11-year solar cycle. Increased F10.7 indicates higher solar UV forcing with more energy absorbed in the upper atmosphere. The geomagnetic activity Kp index is used to specify forcing by the high-latitude convection electric field resulting from the interactions between the solar wind and Earth's magnetic field that leads to Joule heating in the ionosphere and thermosphere. A high Kp index is also an indicator of extra auroral particle precipitation heating into the ionosphere and thermosphere. All these external energy sources increase the temperature in the thermosphere and increase neutral density at a fixed altitude above the heat sources. Compared to prior events with perigees less than 275 km, the F10.7 and 2-day integrated Kp are significantly higher for the February launch. Note that the response of neutral density is not linearly proportional to these indexes. The Kp value is a quasi-log scale, so the thermospheric expansion at the lower altitude for this event is expected to be significantly larger than any prior Starlink launches.

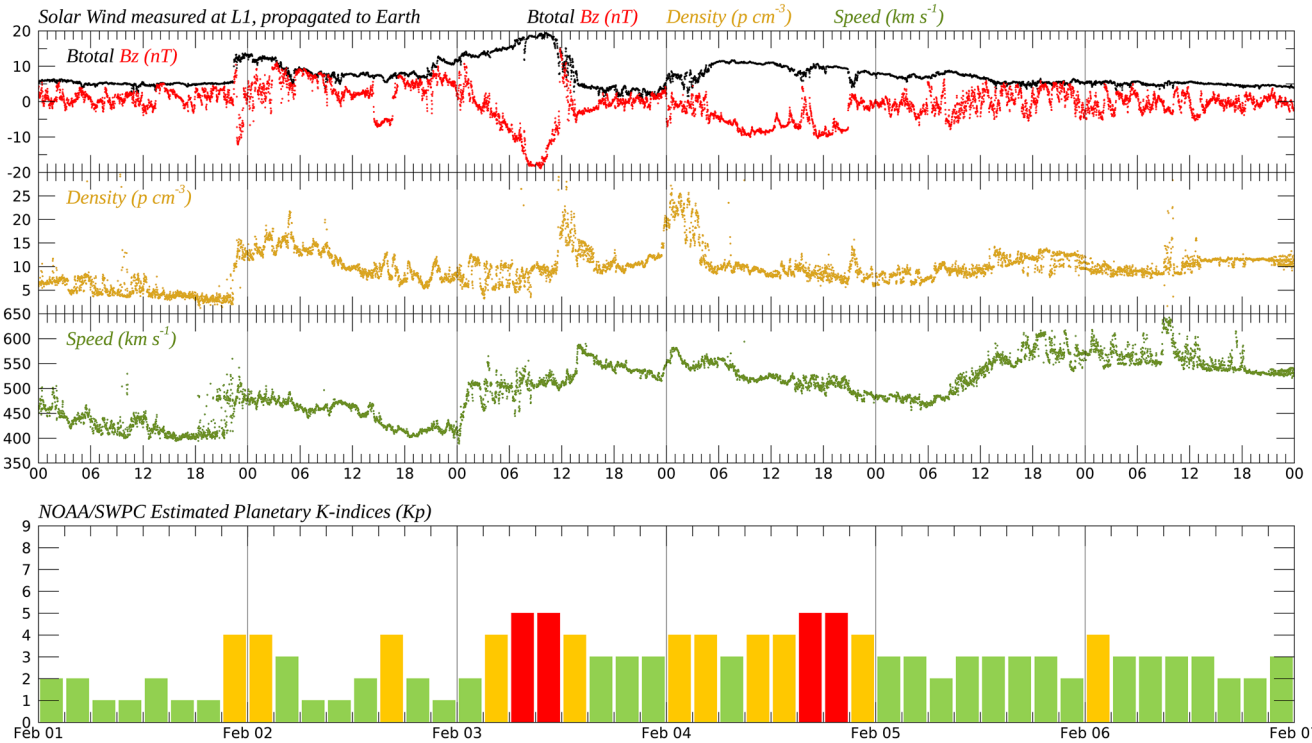

Figure 1. Kp index and solar wind parameters (magnetic field, density, and speed) for the February space weather event.

In the following sections, we first describe in Section 2 the numerical models used to estimate neutral density in this study. Section 3 provides details of space weather forecasts from SWPC for this space weather event. In Section 4, we examine the neutral density estimation based on the WAM-IPE and empirical models as well as their comparisons with satellite measurements. Section 5 provides a summary and some insights for future development of neutral density products based on lessons learned from this event.

2. Numerical Models for Neutral Density Estimations

The study focuses on analyzing the operational outputs from the WAM-IPE to demonstrate the importance of a physics-based whole atmosphere model on estimating the neutral density environment. WAM-IPE provides neutral atmospheric parameters from the ground to the upper thermosphere at around 500 km (e.g., Fang et al., 2016, 2018; T. J. Fuller-Rowell et al., 2008). With the proper assumption of helium in the exosphere, the model outputs can be extended all the way to 1,000 km. WAM was developed based on the spectral version of the National Centers for Environmental Prediction Global Forecast System used for medium-range numerical weather prediction. The WAM system is used to quantify the impact of lower atmosphere weather on the upper atmosphere and ionosphere, as well as the response to solar and geomagnetic activity. To follow real lower atmosphere weather events, data assimilation in the WAM lower atmosphere (WDAS) was developed with a modified version of the gridpoint statistical interpolation three-dimensional variational data assimilation system, with Incremental Analysis Updates (IAU) to spread the increments over the 6-hr assimilation window. IAU avoids using digital filters which adversely affects wave propagation into the thermosphere. The thermospheric parameters calculated by WAM are fed into IPE for calculating the responses in the ionosphere. The ESMF 3D re-gridding capability is used for exchanging the information. IPE is a time-dependent and global three-dimensional model that provides densities, temperatures, and velocity of ions and electron from 90 km to several Earth radii (Maruyama et al., 2016). The International Geomagnetic Reference Field coordinate system is used to accurately represent Earth's magnetic field. The field-line calculations are based on the Field Line Interhemispheric Plasma (FLIP) model (Richards, 2013; Richards & Torr, 1996). The ExB transport is applied zonally and meridionally across Earth's magnetic field. The magnetic field line or flux-tube coordinate system is designed for seamless perpendicular plasma transport pole-to-pole. In the operational setting, both models use the

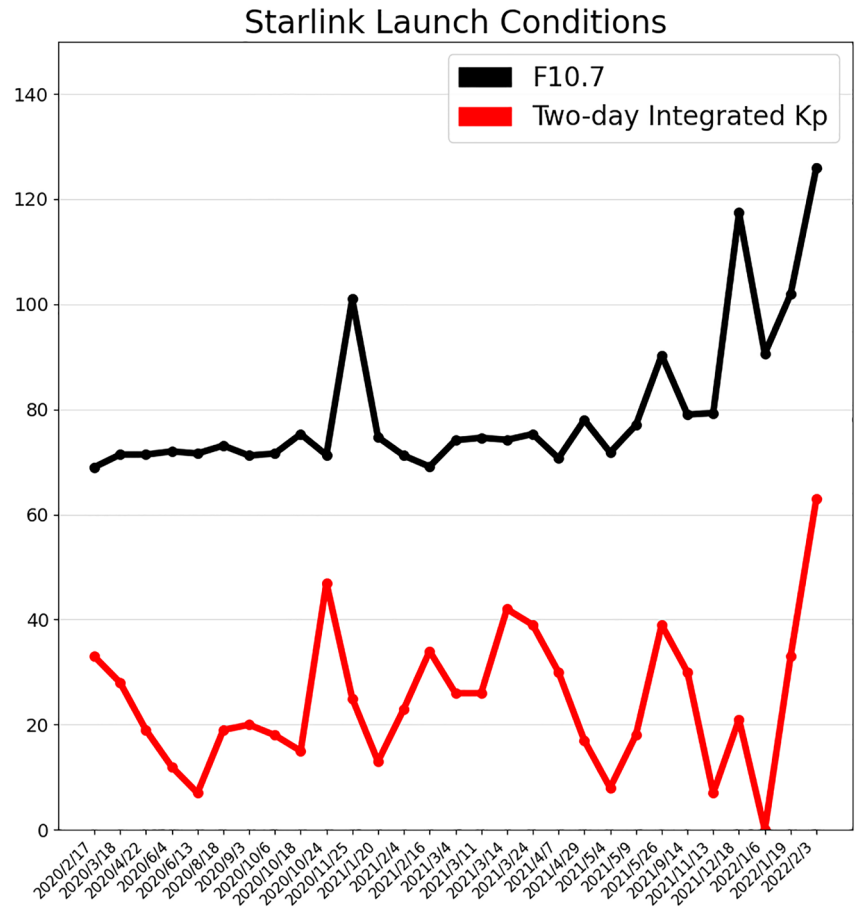

Figure 2. F10.7 and 2-day integrated Kp for all SpaceX Starlink launches that went into an orbit with perigees lower than 275 km.

Weimer empirical ion convection model and TIROS auroral empirical model, both driven by the solar wind data, to specify the external energy input from the magnetosphere. In the current concept of operation, WAM-IPE is run four times daily, providing 2-day forecasts. Observed solar wind parameters are used whenever observational values are available. Lower atmospheric data assimilation in only carried out twice daily to maintain stability of the coupled model. As the model also provides a 2-day forecast when observed space weather drivers are unavailable, the forecasted 3-hr Kp and daily F10.7 issued by SWFO are ingested into the model, and used to estimate solar wind parameters. Note that in this study, only WAM-IPE's operational outputs driven by the real-time solar wind are used to analyze the neutral atmosphere environment that Starlink satellites experienced and to estimate the geomagnetic storm impact on the neutral density variability. As it will be demonstrated in the next section, the forecast portion of the simulations rely highly on the predictions of external drivers associated with the CME eruption direction and solar wind speed, with which still exist large uncertainties under the current capabilities, and are thus not included in this analysis.

Simulations using multiple empirical neutral atmosphere models including NRLMSISE-00 (Picone et al., 2002, hereinafter referred as MSIS-00), the updated version of MSIS-00 model the NRLMSIS v2.0 (Emmert et al., 2021, hereinafter referred as MSIS v2.0), and Drag Temperature Model (DTM2020, Bruinsma & Boniface, 2021) are also examined. These empirical models describe atmospheric temperature, composition, and mass density based on various in-situ or remote sensing observations of the neutral atmosphere. The MSIS-00 and MSIS v2.0 are driven by F10.7 and ap while the DTM2020 is driven by F10.7 and Kp indexes. The values of all these indexes are obtained from SWPC's real-time database as would be used in operations. Based on Bruinsma and Boniface (2021), the DTM2020 densities are on average 20%–30% smaller than those of DTM2013 (Bruinsma, 2015), NRLMSISE-00 and JB2008 (Bowman et al., 2008). The research version of DTM2013 model

is more accurate, but it uses the indices F30 and the hourly Hpo (Jackson et al., 2020), which are not yet accredited operationally.

Also note that the MSIS v2.0 includes an additional license restriction for commercial usage. Therefore, the MSIS-00 is the only neutral density model that is being used by the Starlink team for all the satellite drag estimation under both the geomagnetic quiet and storm conditions. MSIS-00 is also widely used by various satellite operators for drag estimations and by ground-tracking systems for space situational awareness and space traffic coordination. Neutral density differences between WAM-IPE and these empirical models shown in this study not only provide useful insights for the unforeseen Starlink satellite loss event, but also suggest the importance of a physics-based neutral density model in estimating the satellite drag.

3. Space Weather Forecast for the Event From SWPC

The SWFO at SWPC supports full 24/7 operations. SWFO forecasters issue real-time warnings and alerts for customers, including those in the power grid, aviation, communication, and navigation industries. Rocket launch sites in the US also often contact SWFO prior to a launch for situational awareness. NOAA supports various real-time observations including solar images at different wavelengths and solar wind parameters measured at the L1 point by the DSCOVR and ACE satellites. Other observations in space and from the ground include the NOAA GOES satellite measurements in Geostationary orbit, solar radio wave signatures, the radiation environment near Earth, magnetic field measurements in the space environment and on the ground and ionosphere measurements. Observations are made by NOAA assets as well as from satellites and instruments supported by partner organizations such as NASA, NSF, USGS, and the USAF. Combining these real-time observations and various numerical models that propagate solar events to the magnetosphere, ionosphere, and thermosphere, SWPC's forecasters utilize all the information to issue alerts and warnings and to forecast the impact of space weather conditions several days in advance. Typically, SWFO provides a 3-day forecast of geomagnetic activity via an estimated planetary Kp index and F10.7. The 3-day Kp forecasts are updated at 00:30 and 12:30 UTC daily unless they are further amended to reflect an ongoing geomagnetic storm. F10.7 is updated at 21:00 UT with the observed values each day. The quasi-log scale Kp index is a three-hour index and can be converted into the linear-scale ap index to drive various empirical models (e.g., MSIS-00 and DTM) and parameterization schemes used in physics-based thermosphere and ionosphere models. The forecast F10.7 and Kp from SWFO are continuously ingested into the operational WAM-IPE model to provide a 2-day forecast of ionosphere and thermosphere conditions (https://www.swpc.noaa.gov/products/wam-ipe). Although the global 400 km neutral density forecast from WAM-IPE is currently displayed as an operational product on the SWPC website, SWFO does not issue specific alerts or warnings for satellite drag based on WAM-IPE results at this time.

Several tools are used at SWFO to predict Kp values based on estimations of possible CME impacts at Earth. Difference imaging of the solar corona from coronagraph telescopes on the SOHO and STEREO A spacecraft reveal explosive CME structures, observed concurrently from two different vantage points in the Heliosphere. These images are then synthesized within a 3-dimensional CME Analysis Tool (SWPC_CAT) to calculate the CME trajectory: the direction of propagation, angular extent, and speed. These CME properties are then fed into the Wang-Sheeley-Arge Enlil model (WSA-Enlil) to estimate the full CME propagation through the Heliosphere, from Sun to (a possible interaction with) Earth. WSA-Enlil is a large-scale, time dependent, 3-dimensional MHD model of the heliosphere, used by SWFO to provide 1–4 days advance warning of solar wind structures and Earth-directed CMEs that cause geomagnetic storms.

Figure 3 shows the WSA-Enlil prediction of solar wind propagation from the Sun to Earth for the 29 January CME. The figure shows the arrival of the CME structure at Earth at 00:00 UTC on the 2 February. Utilizing this, and other WSA-Enlil model runs, G2 (moderate) and G1 (minor) Geomagnetic storm watches were issued for 2 and 3 February, respectively, as shown in Figure 4 (denoted by the two green horizontal stripes). Based on SWPC's space weather scale for Geomagnetic storms (https://www.swpc.noaa.gov/noaa-scales-explanation), the Kp index will reach 6 and 5 under G2 and G1 storms, respectively. Under G2 conditions, general guidance states that corrective actions to orientation may be required by spacecraft operators and possible changes in orbital drag are predicted. For G1, minor impact on satellite operations is possible.

As a result of the SWFO assessment, the following sentences were included in the 3-day forecast issued at both 00:30 and 12:30 UTC on 1 February.

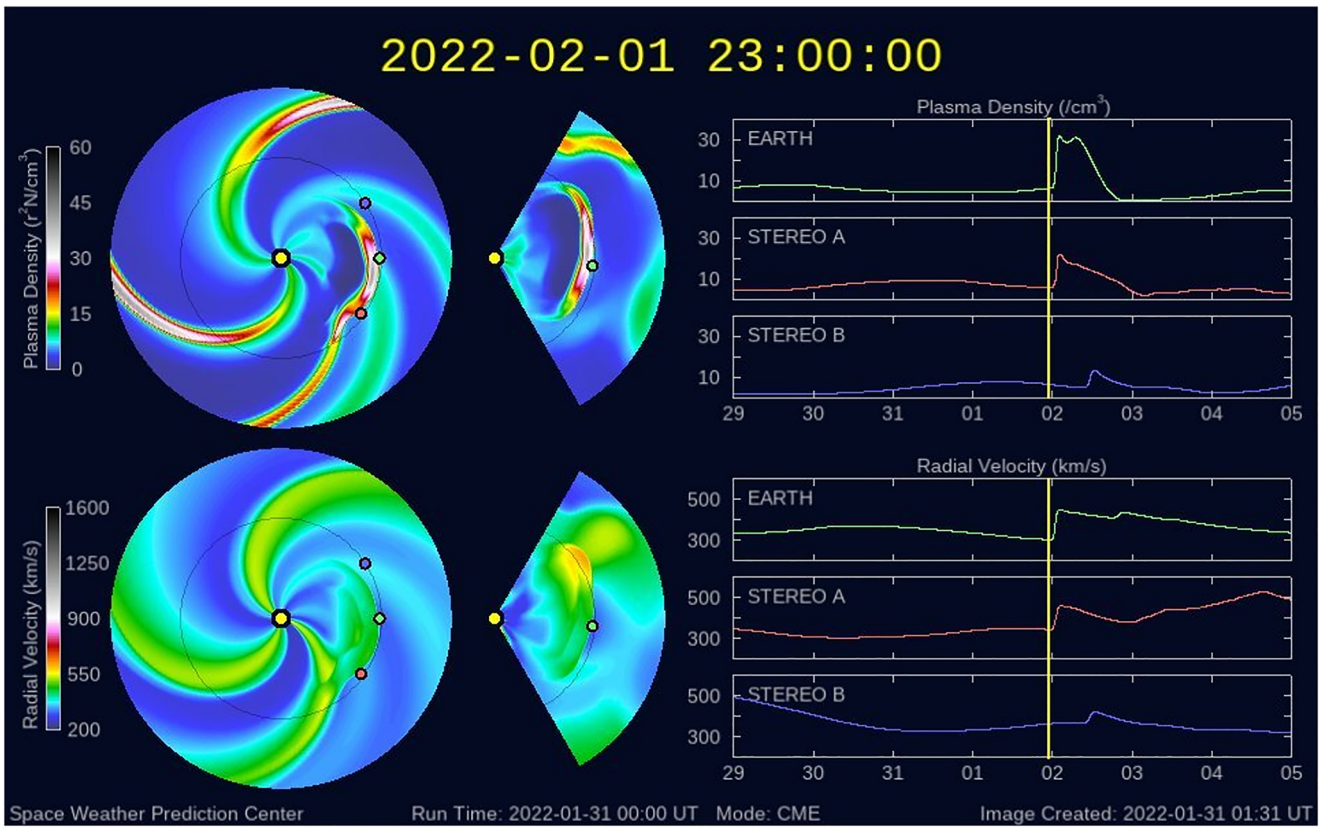

Figure 3. The Wang-Sheeley-Arge Enlil prediction of solar wind plasma density (top panels) and velocity (bottom panels) for a model run with background solar conditions starting at 00:00 UT on the 31 January 2022. Utilizing this prediction and other information, Space Weather Forecast Office expected that the arrival time of Coronal Mass Ejection at Earth should be around 00:00 UT on 2 February 2022. In this plot, the arrival time at Earth (green circle), Stereo A spacecraft (just inside 1AU, red circle), and Stereo B spacecraft (decommissioned, blue circle) are included.

"A G2 (Moderate) geomagnetic storm is likely on 2 February due to the anticipated arrival of a CME from late 29 January. Any CME effects are likely to linger into 3 February at G1 (Minor) storm levels."

The red line in the right panel of Figure 4 shows the Kp values that were forecasted by SWFO at 00:30 UTC on 1 February. In comparison to the actual observations shown in the same figure (black line), the response to the solar wind propagation was more variable with three separate increases of Kp, and the peak did not occur until 3 February and was smaller than predicted. Predictions of CME arrival time at Earth and the impact on geomagnetic activity and the thermosphere and ionosphere still require significant advances by the research community. Future studies focused on the uncertainties and variability of solar wind/near-Earth interactions will also provide useful information to improve predictions and better quantify the uncertainty in the predictions and the response of magnetospheric activity.

The SWFO forecast provides useful information on how the CME event evolved based on the best knowledge and tools that SWPC has available. SWFO successfully predicted the minor to moderate storm conditions. The forecasted solar and geomagnetic storm conditions are extremely valuable for near-future mission planning and other operations. However, the insufficient measurements between Sun and Earth, deficiencies in our modeling tools, and knowledge gaps in space physics all lead to a prediction error on the actual geomagnetic storm timing. Methods to improve forecasts of the time and intensity of geomagnetic storms remain one of the highest priorities for SWPC and the space weather research community.

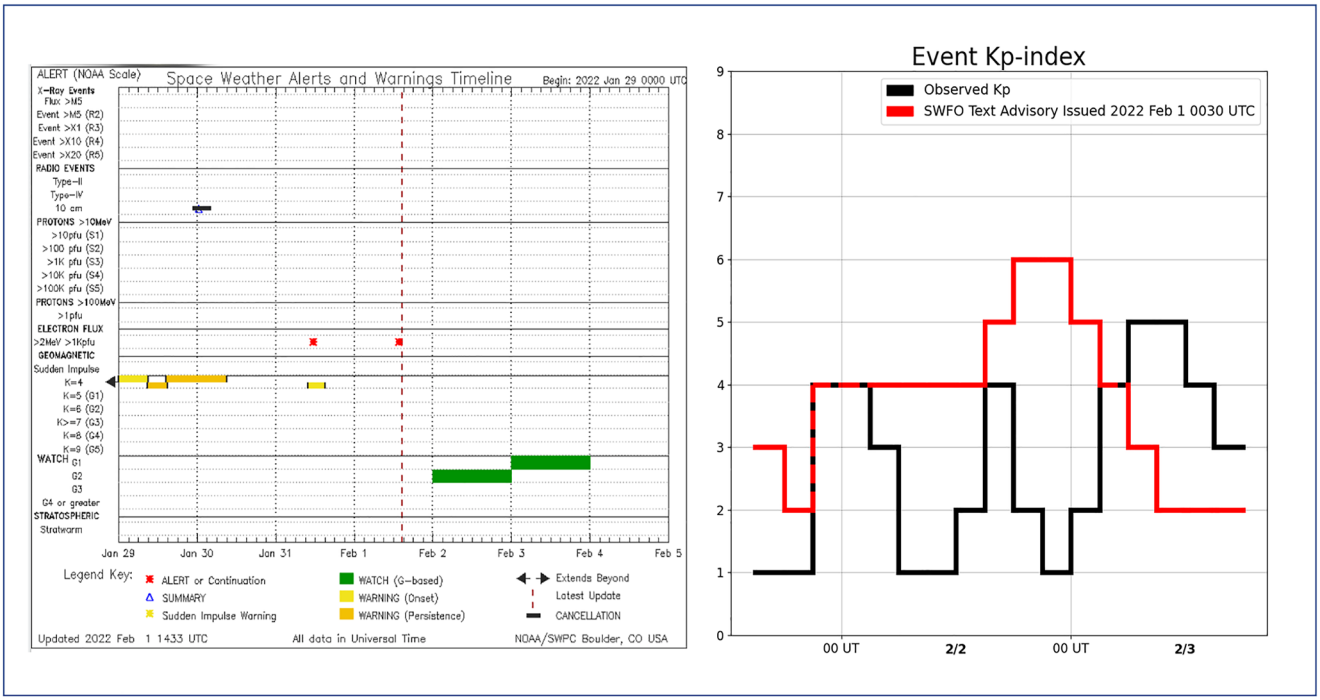

Figure 4. Space weather alerts and warnings issued by Space Weather Forecast Office at 14:33 UTC on 1 February 2022 (left). The two green bars show the G2 and G1 predictions for 2 and 3 February, respectively. Forecasted Kp index issued at 00:30 on 1 February (red line) and observed Kp (black line) are also shown (right). This forecast suggested Kp 5–6 conditions between 15:00 on 2 February and 03:00 UT on 3 February. The observation shows that the peak Kp reaches 5 between 03:00 and 09:00 UT on 3 February.

4. Model Simulation of the Neutral Density Environment

In this section, outputs from the operational WAM-IPE and empirical models are used to analyze the neutral density environment during the event. The differences in neutral density results between WAM-IPE and MSIS-00 provide some estimation of possible differences in satellite drag that the Starlink team had not anticipated. In these simulations, the WAM-IPE was driven exclusively by the daily F10.7 and 1-min cadence solar wind and IMF parameters, while MSIS-00 and other empirical models were driven by daily F10.7 and ap values converted from the real-time estimated 3-hr Kp. In WAM-IPE, the neutral density is calculated by summing the mass densities of atomic oxygen (O), molecular oxygen (O_2), and molecular nitrogen (N_2) at fixed altitudes. All model outputs are standardized to 10-min cadence. The native WAM-IPE neutral atmosphere parameters are prescribed on hybrid-sigma pressure levels, and have been interpolated into a fixed-height grid with 10 km altitude interval. The WAM-IPE output longitude and latitude resolution is 4° and 2°, respectively. The same three-dimensional grid is used to produce an equivalent output from the empirical models. For use in one-minute cadence satellite orbit sampling, these outputs are further interpolated in all four dimensions.

Figure 5 shows the global neutral density and density anomalies from MSIS-00 and WAM at 11:50 UT on 4 February at 210 km. The anomalies were calculated by subtracting the current values from the 10-day averaged densities from each model at the same UT. Note that the color scales are different for MSIS-00 and WAM absolute densities. The comparison shows that WAM density prediction is much higher than MSIS-00 during the event. Comparisons of global mean density (not shown here) also suggests that the WAM neutral density was consistently higher than MSIS-00 throughout 3 and 4 February at all altitudes. The WAM density also displays significantly more small-scale perturbations and structure than MSIS-00. In the anomaly plots, WAM suggested at least a 50% density increase in most regions and more than 100% increase in some specific areas but MSIS-00 only showed up to 20% enhancement in the density.

The small-scale spatial variability and structure shown in WAM density are associated with the realistic atmospheric weather patterns in the lower atmosphere that are expected in all our simulations, and the time-dependence in the response and recovery to energy injection enabled by the physical model. Previous studies comparing

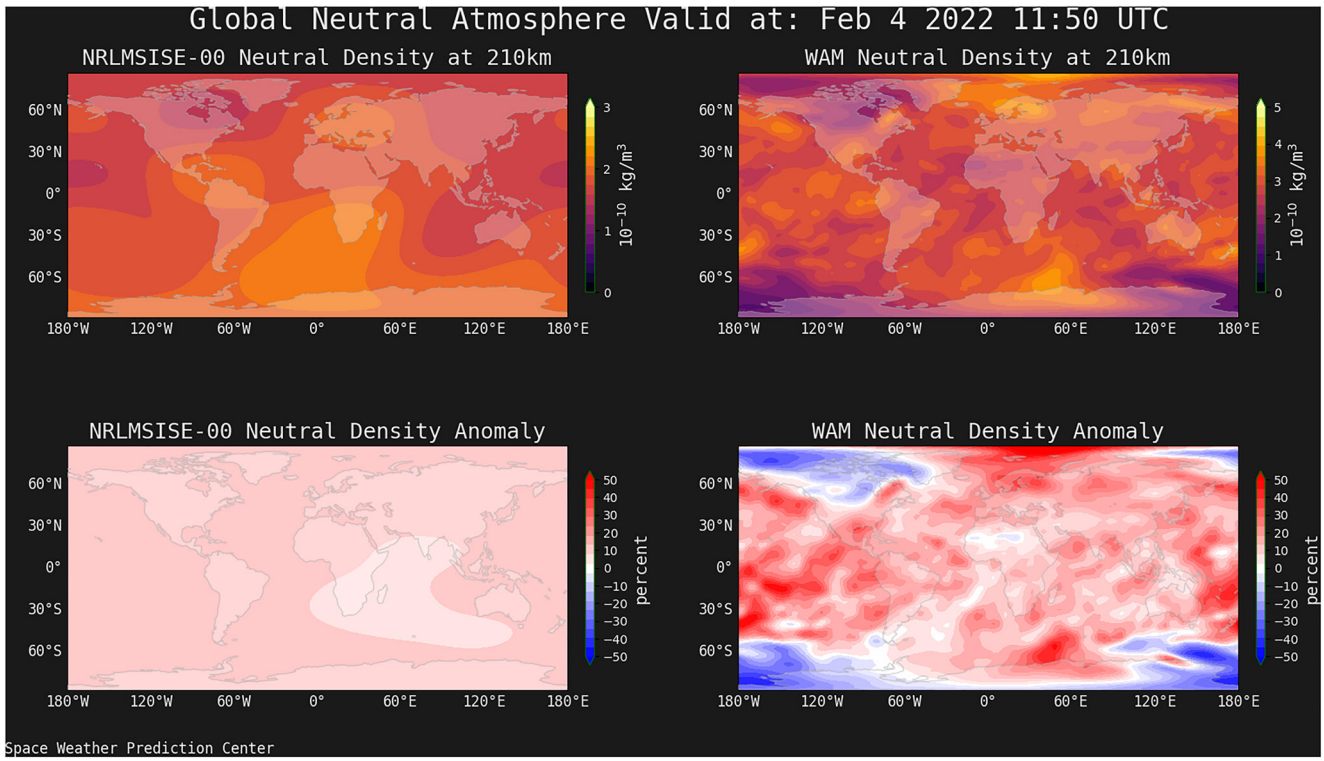

Figure 5. Global neutral density and density anomaly at 210 km simulated by MSIS-00 (left) and coupled Whole Atmosphere Model and Ionosphere Plasmasphere Electrodynamics (right) at 11:50 UTC on 4 February 2022.

model results with satellite accelerometer observations (CHAMP, GRACE, and GOCE) have demonstrated good agreement in the global seasonal/latitude structure along orbits as well as density enhancements during storms with a wide range of storm intensity (T. J. Fuller-Rowell et al., 2021, 2022). Our previous study also demonstrated that the WAM thermosphere is sufficient to produce significant ionospheric day-to-day variability that is comparable to observations (Fang et al., 2018). Therefore, the variability predicted by WAM for the event likely provides a much more realistic environment compared to those shown in MSIS-00. Empirical models driven by the 3-hr Kp or ap may predict mean levels, but tend to be smooth due to the numerical fitting and lack of data. The physics-based model, on the other hand, clearly depicts structure induced by waves from the lower atmosphere and structure induced by the time dependence of the solar/magnetospheric drivers used to drive the model. Prior study has demonstrated the importance of utilizing high cadence solar/magnetospheric drivers in specifying Joule heating for better neutral density estimation in the physics-based model (Fedrizzi et al., 2012). All these variabilities could add a 30%–50% variation in density locally. The impact of this structure and variability on satellite orbit projections needs to be further investigated.

The detailed orbit information for all satellites from this launch and prior launches were provided by the Starlink team. Figure 6 shows the orbits of two satellites (#3165 and #3419) that were launched along with the other 49 satellites on 3 February and did survive the higher neutral density environment associated with the geomagnetic storm. Minor data gaps can be seen in the figure. Even though all the Starlink satellites were deployed together, the onboard orbit determination estimates showed different altitudes for these two satellites. For satellite #3165, due to significantly increased drag and instability on orbit, the thrust applied for orbit raising was not initiated until 7 February. Thus, within the 5-day period, the perigee of the satellite remained low (~200 km) and only started to increase to a slightly higher altitude toward the end of the fifth day. The apogee also reduced from ~330 to <300 km. On the other hand, the orbit raising process for satellite #3419 was able to start from early in the UT hours on 6 February. Based on the altitudes in this plot, the perigees also showed smooth increases as orbit-raising thrust was applied.

Using the provided longitudes, latitudes, and altitudes for these satellites, the neutral density obtained from WAM and MSIS-00 are sampled along the orbits. The unstable periods at the beginning of the orbits before 12:00 UT on

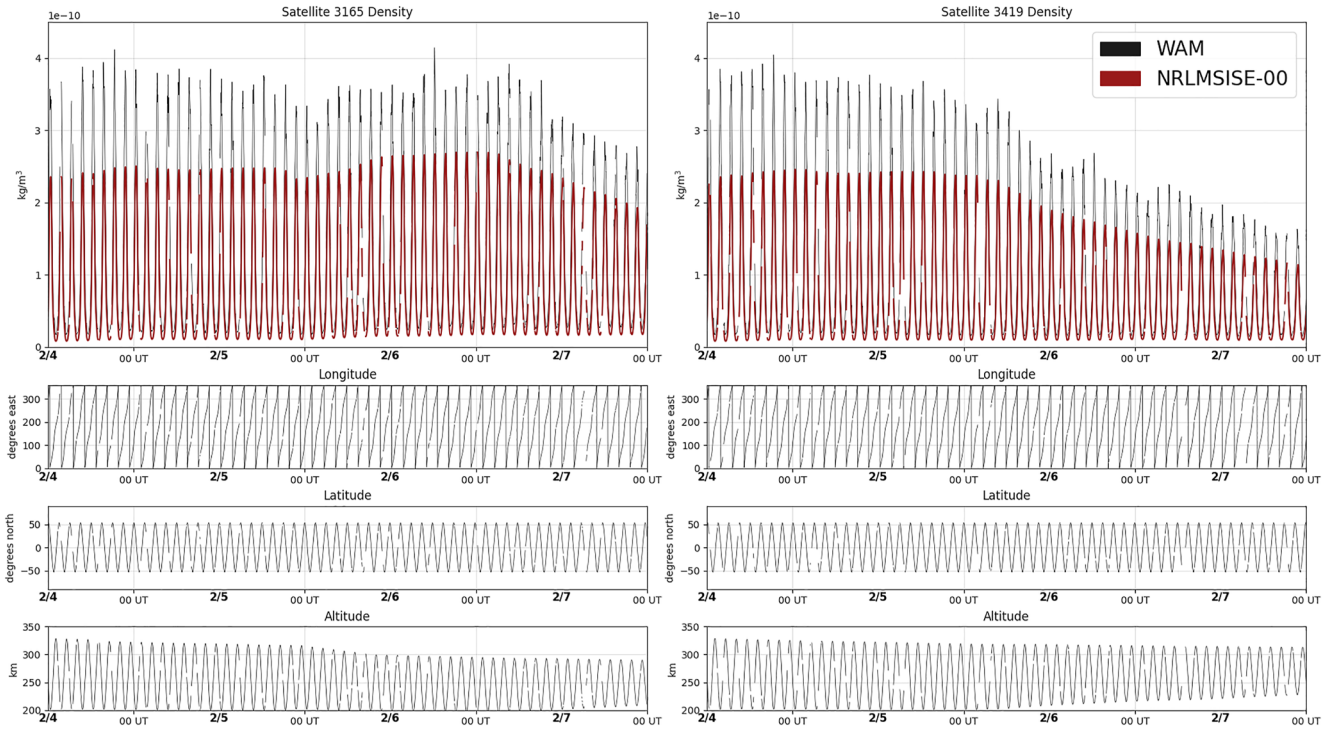

Figure 6. Neutral density sampled along orbits of two Starlink satellites (3165 and 3419) from coupled Whole Atmosphere Model and Ionosphere Plasmasphere Electrodynamics (black) and MSIS-00 (brown) global densities. The locations for these satellites in longitude, latitude, and altitude are also included.

4 February are omitted in the plot. Since all the satellites were released together and stayed in relative proximity, for an initial period the density results are very similar on 4 and 5 February for all 11 satellites that survived. With the faster orbit raising leading to increased perigee altitudes and calmer space weather conditions after 5 February, significant density decreases at perigees can be seen for satellite #3419.

Figure 6 shows that the WAM densities are higher than MSIS-00 densities throughout these orbits. Overall, during the period, WAM densities are roughly 40%–80% higher at perigees and 60%–100% higher at apogees compared to those from MSIS-00. Prior to all the launches, the Starlink team carries out satellite drag estimations based on MSIS-00 neutral density, which is driven by the 3-hr ap index (linear scale for geomagnetic activity, which can be directly derived from the 3-hr Kp index). Before the launch on 3 February, the team expected a roughly 50% increase in density based on the MSIS-00 simulation for the predicted storm. However, the geomagnetic storm perturbations continued into 4 February and the neutral density enhancement lasted until the early UT hours of 5 February. Based on further analysis carried out by the Starlink team, the at least 50% higher neutral density WAM suggested is approximately what was required to initiate safe hold for Starlink satellites. The Starlink team has implemented several system upgrades to ensure future low insertion missions can accommodate the satellite drag with increased solar and geomagnetic activities in solar cycle 25.

For both satellites in Figure 6, it is also shown that the changes in the neutral density at perigee from 4 to 7 February from WAM are much larger than the changes estimated by MSIS-00. WAM densities clearly show a much stronger response to the geomagnetic storm. Compared to the 3-hr ap that drives the MSIS-00 empirical model, a physics-based model driven by high cadence (1-min) solar wind parameters such as WAM, provides a more realistic specification of both the energy inputs in the thermosphere and the neutral density response. The storm-time responses in WAM have previously shown good agreement with in-situ accelerometer measurements during the 2013 and 2015 St. Patrick Day storms as well as the 2003 November storm (T. J. Fuller-Rowell et al., 2021). The comparison demonstrates the benefits to the Starlink team, or other satellite operators, to consider including WAM forecasts in their future decision-making process.

Similar to Figures 6 and 7 includes results of neutral density based on simulation outputs from two other empirical models, MSIS v2.0 and DTM. The results confirm that at these orbits WAM produces significantly larger

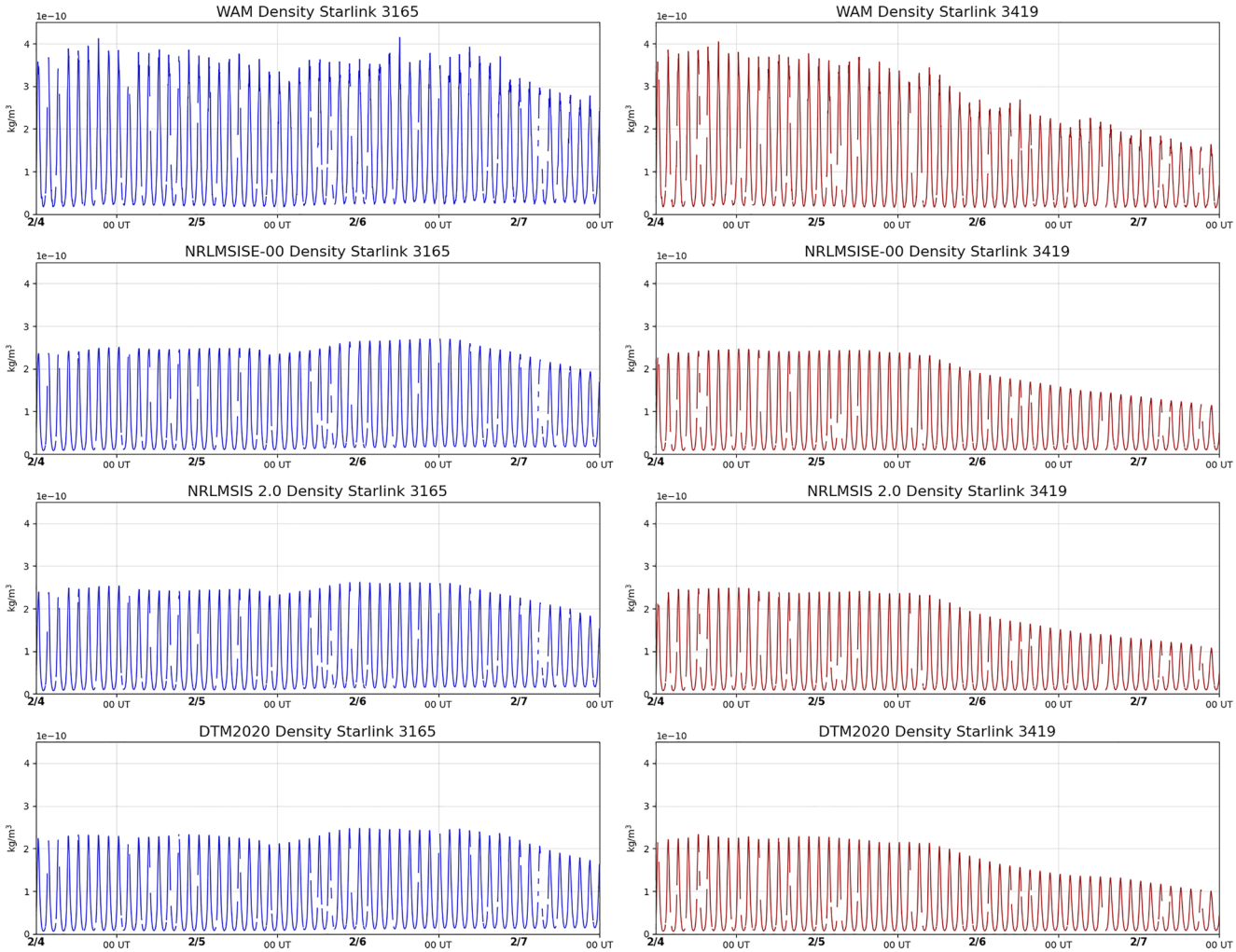

Figure 7. Similar to Figure 6 but the neutral density sampled along orbits of two Starlink satellites (3165 and 3419) using MSIS v2.0 and DTM are also included.

density compared to the empirical models. The MSIS v2.0 density is slightly higher than MSIS-00. Both MSIS results are also higher than DTM. Comparing the density anomalies from these models for the event (not shown here), MSIS v2.0 shows a similar enhancement as those in WAM (up to 50% density increase). MSIS-00 and DTM, on the other hand, do not show pronounced density enhancement associated with the geomagnetic storm. These results again demonstrate the deficiency of empirical models in capturing neutral density responses under the geomagnetic storm conditions.

To estimate the reliability of WAM neutral density results, simulations are further compared with the onboard drag estimates obtained from Starlink satellites. The satellite telemetry data provides not only the satellite locations and satellite conditions, but also the satellite attitude, drag coefficients, and drag acceleration estimated by the onboard orbit determination algorithm based on a Kalman filter. The algorithm was designed based on methods described in the book edited by Tapley et al. (2004). The Kalman filter uses Global Positional System position, velocity and precise time, spacecraft mass properties, along with information from various orbital models (gravity, solar radiation pressure, drag etc.) to continuously estimate orbital information for use in on-board navigation and collision avoidance. The satellite attitude estimation is rather accurate and has been validated both in ground testing and through over 4,000 satellite years of on-orbit operations. The drag coefficient and acceleration are estimated by the Kalman filter, which runs at 10 Hz continuously. Satellite drag varies strongly as a function of the neutral thermospheric density and the satellite ballistic coefficient. Aerodynamic drag acceleration ($\overline{a}_D$) is expressed by the equation below in terms of atmospheric density (ρ), drag coefficient (C_D), cross-sectional area (A), spacecraft mass (M), and the spacecraft velocity relative to the atmosphere (V_r). Using the drag acceleration and drag

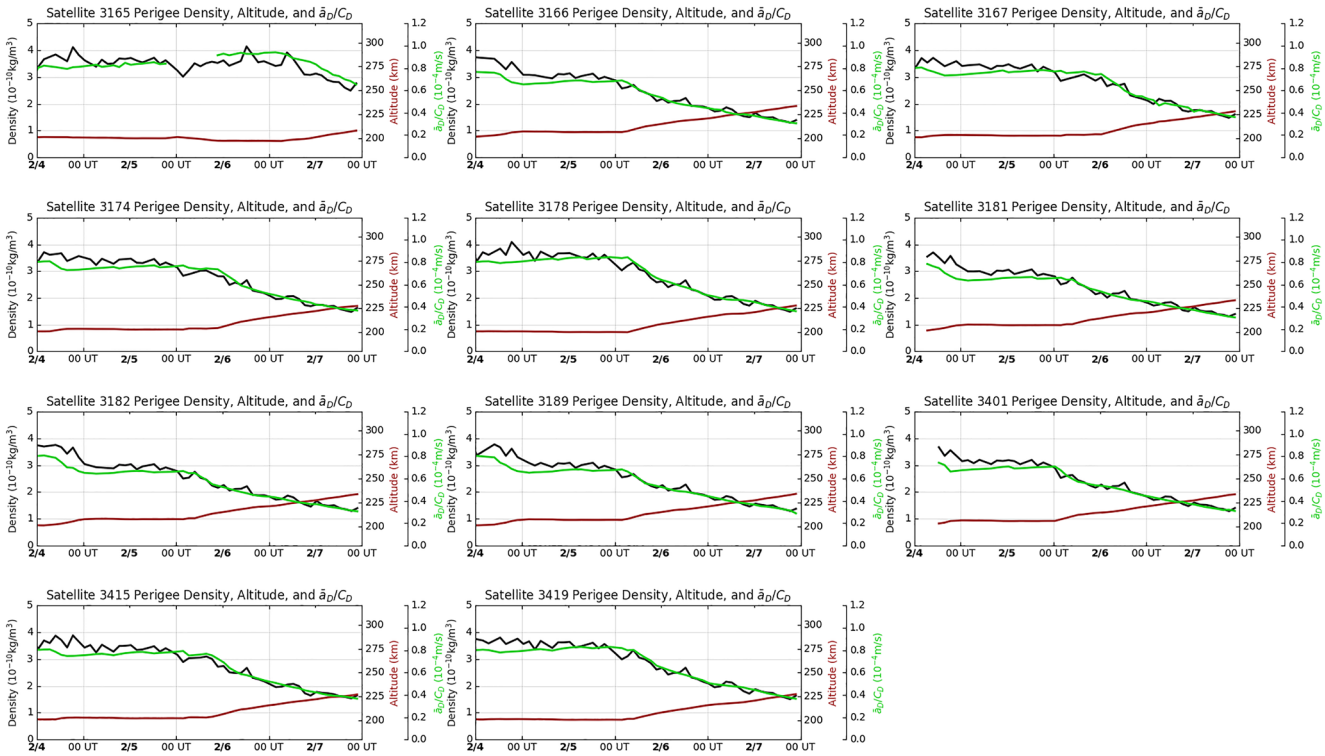

Figure 8. Neutral density sample at perigee for all surviving Starlink satellites for this launch based on coupled Whole Atmosphere Model and Ionosphere Plasmasphere Electrodynamics density (black), neutral density proxy along the orbit measured by the Starlink satellites (green, see main text for more details), and satellite altitudes (red).

coefficient derived by the Kalman filter, we calculate the neutral density proxy along the orbit (ρ_{obt}) through dividing the drag acceleration ($\bar{a}_{\mathrm{D}}$) by drag coefficient (C_{D}) along the orbit for each satellite. The obtained ρ_{obt} should be linearly proportional to the neutral density that each satellite experienced along the orbit. Periods when satellites were tumbling or unstable with large body rotation rate (>0.005 rad/s) are removed from the data set.

$$\bar{a}_{\mathrm{D}} = -\frac{1}{2}\rho\frac{C_{\mathrm{D}}A}{M}V_{\mathrm{r}}^2 = C_{\mathrm{D}} * \rho_{\mathrm{obt}}$$

$$\rho_{\mathrm{obt}} = \frac{1}{2}\rho\frac{A}{M}V_{\mathrm{r}}^2$$

Figure 8 shows the comparisons of WAM density (black lines) and ρ_{obt} from Starlink satellites (green lines) at satellite perigees (red lines) of each orbit of the 11 surviving satellites. The comparisons show that variations of WAM density with height show a good agreement with changes in ρ_{obt} from Starlink satellites. The decreased WAM neutral density with increased perigee altitudes follows the slope of the satellite observations. Compared to the Kalman filter results, WAM density appears to have more variability throughout the period for all satellites. To better understand these differences, in the future it is necessary to carefully estimate neutral density along the orbit. Compared to other satellites, satellite #3165 remains at low altitudes for many days due to the unstable conditions, the density estimations at perigees provided by the on-board calculation also showed different behavior from others.

There have been more than 30 SpaceX launches since November 2019 specifically for deploying the Starlink system. The Starlink system version 1.5 has been in operation since September 2021. To investigate the differences in the neutral density from this February 2022 event with prior deployments, we further compare the neutral density estimated from the WAM-IPE during two other launches on 18 December 2021, and 6 January 2022. The insertion orbit on 18 December 2021 for satellite Group 4-4 is 340 × 208 km with 53° inclination launched at Vandenberg Air Force Base in California and on 26 January 2022 for satellite Group 4-5 is 350 × 210 km with 53° inclination launched at Kennedy Space Center in Florida.

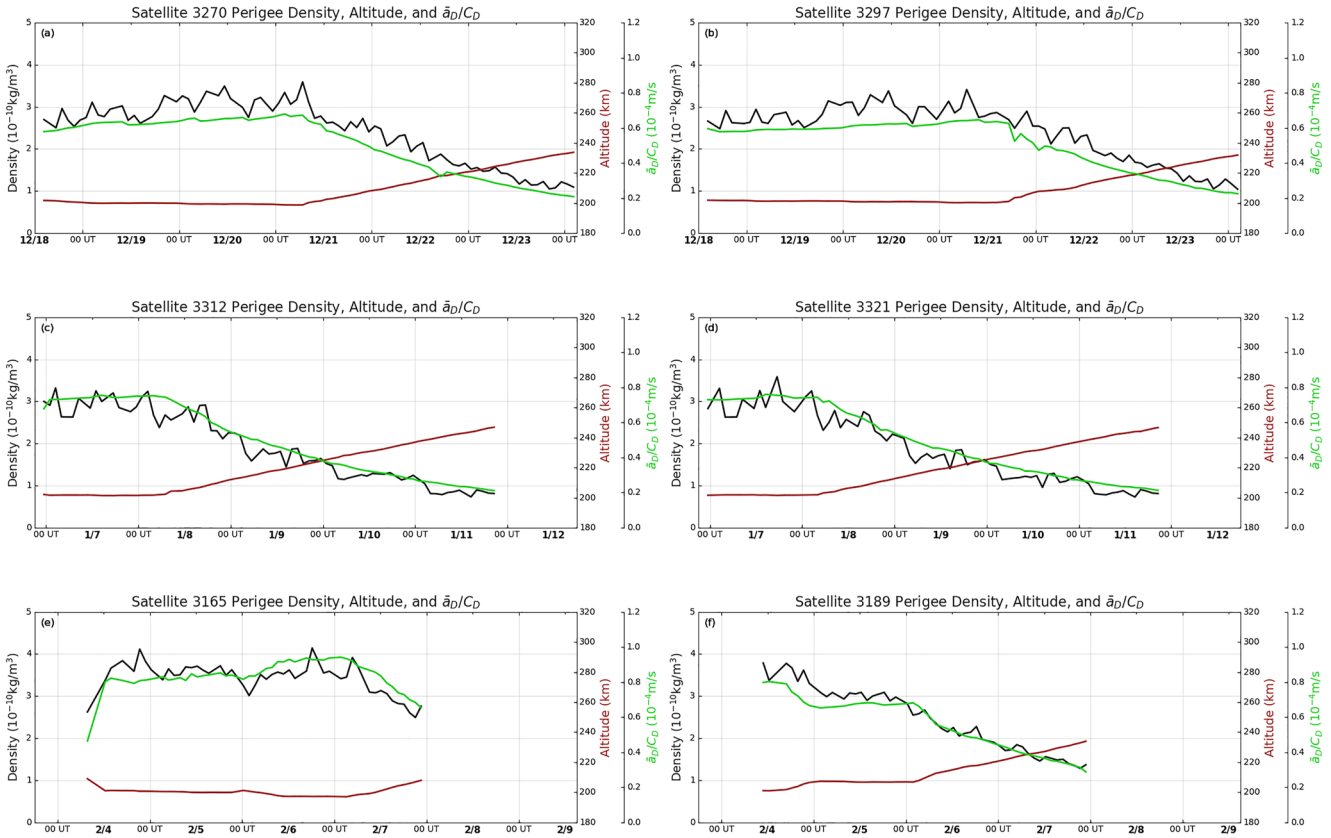

Figure 9. Neutral density at perigees for Starlink satellites from different launches based on coupled Whole Atmosphere Model and Ionosphere Plasmasphere Electrodynamics density (black), neutral density proxy along the orbit measured by the Starlink satellites (green), and satellite altitudes (red). (a, b) Satellites #3270 and #3297 are from the Group 4-4 launch, (c, d) satellites #3312 and #3321 are from the Group 4-5 launch, and (e, f) satellites #3165 and #3189 are from the Group 4-7 launch.

In Figure 9, similar to the previous figure, the satellite locations provided by the Starlink team from different periods are used. The plot shows the sampled neutral densities from operational WAM-IPE outputs and neutral density proxy from Starlink satellites at perigees for time periods right after three different launches including the 3 February event. Two satellites are selected from each period: satellites #3270 and #3297 are from the Group 4-4 launch (Figure 9a and 9b), satellites #3312 and #3321 are from the Group 4-5 launch (Figure 9c and 9d), and satellites #3165 and #3189 are from the Group 4-7 launch (Figure 9e and 9f). In these plots, the starting time in each subplot matches the time of the satellite launch. As previously described, the orbit-raising maneuvers typically start within 2 days after the launch date in most cases. All the initial perigees for these satellites are at around 200 km. Comparing the initial neutral densities experienced for these satellites across the three different periods, it is clearly shown that the values for Group 4-7 are much larger at the initial perigees compared. For Starlink satellites, after starting the orbit raising process, the electrical propulsion applies thrust at apogees in order to raise the perigees as soon as possible. In the February case for satellite #3165, the high background neutral density due to the long-lasting geomagnetic storm further increased the satellite drag and reduced satellite stability, and the orbit-raising maneuver was not able to be successfully be initiated until 7 February. The difficulty in maintaining a stable attitude to apply thrust appears to be an extremely challenging problem related to the geomagnetic storm events. The instability of satellites associated with the strong thermospheric drag eventually led to the loss of many other Group 4-7 satellites.

5. Forecasting Capability and Future Steps

For this space weather event, a series of Earth-directed and partially Earth-directed CMEs were detected by multiple spacecraft and ground-based observations between 29 and 31 January 2022. The CMEs were not particularly strong and SWPC forecast the CMEs to arrive at Earth as early as 2 February 2022. During this event, the CME

arrival generated geomagnetic storms with Kp 5 for more than 6 hr on both 3 and 4 February. Even though this is considered a minor to moderate geomagnetic storm, the external energy injection into the thermosphere still caused thermospheric expansion that significantly enhanced the neutral density in the VLEO environment. SWPC had several watch, warning, and alert products in effect for this event beginning 31 January and continuing through 5 February. While this information provides useful and actionable guidance, improvement of the forecast skill on CME arrival time and better estimation of the CME impact on Earth's upper atmosphere still require significant research efforts to achieve the accuracy, along with confidence levels, that is urgently needed.

The WAM-IPE, implemented in July 2021, is SWPC's newest operational space weather model. Driven by the real-time solar wind observations, WAM-IPE captured the enhanced neutral density that globally increased satellite drag in early February 2022. Based on WAM-IPE simulations, the neutral density enhancement for this event ranged from 50% to 125%, depending on location and altitude. Such a magnitude of density increase is very common for a minor to a moderate geomagnetic storm. Thus, with increasing solar activity in the current solar cycle 25, the frequency of neutral density enhancement events of a similar magnitude will be very high. This geomagnetic storm event highlighted the need for the satellite industry to utilize improved models for specifying the response of the satellite environment to space weather and to incorporate this information into satellite design and operations.

The study also demonstrated that the neutral density estimated by WAM-IPE at 210 km is significantly higher than that predicted by the empirical models, leading to a level of satellite drag that was not anticipated by the Starlink team. WAM-IPE densities at perigee (200–250 km) agree well with the onboard calculated neutral density proxy provided by Starlink satellites. Using the same orbital data set to derive the orbit-averaged neutral density is a clear next step that will truly take advantage of a large satellite constellation such as Starlink. Developing computationally efficient data-assimilation techniques to utilize the large volume of on-orbit neutral density observations will allow SWPC to improve neutral atmosphere nowcasts. The current WAM-IPE forecasts are driven by F10.7 and Kp forecasts (not shown in this study), which in turn rely on better predictions of solar activity and the solar wind impacting the Geospace environment. Commercial satellite operators receive general forecasts, watch, warnings, and alerts through NOAA's data and web services, but none are currently specifically focused on satellite drag at LEO. Thus, it is critical for SWPC to establish alerts and warnings for thermospheric density enhancement conditions. This information will certainly become essential when dealing with space traffic coordination in an increasingly crowded space environment during both geomagnetic quiet and perturbed conditions. The Starlink team and other satellite operators obtain space weather data from Celestrak, which provides space weather information from various sources. SWPC is engaging with Celestrak to ensure SWPC's forecasts information will be properly utilized in the community. Through collaboration and engagement, the Starlink team has started to utilize historical WAM-IPE neutral density for their drag modeling as well as to explore the forecast outputs that are currently available to the public. SWPC will continue to work closely with the Starlink team, and others in the spacecraft industry, to expand the current space weather services to provide neutral density alerts and warnings for satellite operators. In addition, the 4-dimensional operational WAM-IPE model predictions, in space and time, can be made available to the orbit propagation community in the near future.

Data Availability Statement

All the data used in this study including modeling results and Starlink satellite data can be found at https://zenodo.org/record/7026474.

Acknowledgments
The NOAA SWPC team greatly appreciates the engagement and data that the Starlink team provided for this study. T.-W. Fang would like to thank the input and suggestions from Dr. Amal Chandran at LASP at the University of Colorado Boulder.

References

Bowman, B. R., Tobiska, W. K., Marcos, F., Huang, C. Y., Lin, C. S., & Burke, W. J. (2008). A new empirical thermospheric density model JB2008 using new solar and geomagnetic indices. In *AIAA/AAS Astrodynamics Specialist Conference*. AIAA 2008-6438.

Bruinsma, S., & Boniface, C. (2021). The operational and research DTM-2020 thermosphere models. *Journal of Space Weather and Space Climate*, EDP sciences, *11*, 47-1–47-15. https://doi.org/10.1051/swsc/2021032

Bruinsma, S., Boniface, C., Sutton, E. K., & Fedrizzi, M. (2021). Thermosphere modeling capabilities assessment: Geomagnetic storms. *Journal of Space Weather and Space Climate*, *11*, 12. https://doi.org/10.1051/swsc/2021002

Bruinsma, S. L. (2015). The DTM-2013 thermosphere model. *Journal of Space Weather and Space Climate*, *5*, A1. https://doi.org/10.1051/swsc/2015001

Emmert, J. T., Drob, D. P., Picone, J. M., Siskind, D. E., Jones, M., Mlynczak, M. G., et al. (2021). NRLMSIS 2.0: A whole-atmosphere empirical model of temperature and neutral species densities. *Earth and Space Science*, *8*(3), e2020EA001321. https://doi.org/10.1029/2020EA001321

Fang, T.-W., Akmaev, R., Stoneback, R. A., Fuller-Rowell, T., Wang, H., & Wu, F. (2016). Impact of midnight thermosphere dynamics on the equatorial ionospheric vertical drifts. *Journal of Geophysical Research: Space Physics*, *121*(5), 4858–4868. https://doi.org/10.1002/2015JA022282

Fang, T.-W., Fuller-Rowell, T., Yudin, V., Matsuo, T., & Viereck, R. (2018). Quantifying the sources of ionosphere day-to-day variability. *Journal of Geophysical Research: Space Physics*, *123*(11), 9682–9696. https://doi.org/10.1029/2018JA025525

Fedrizzi, M., Fuller-Rowell, T. J., & Codrescu, M. V. (2012). Global Joule heating index derived from thermospheric density physics-based modeling and observations. *Space Weather*, *10*(3), S03001. https://doi.org/10.1029/2011SW000724

Fuller-Rowell, T. J., Li, Z., Fang, T.-W., Fedrizzi, M., MacCandless, M., Sutton, E., et al. (2021). Neutral density for satellite drag and space traffic management from an operational physics-based model. SA24B-09 presented at 2021. In *AGU Fall Meeting Abstract*. Retrieved from https://ui.adsabs.harvard.edu/abs/2021AGUFMSA24B.09F/abstract

Fuller-Rowell, T. J., Akmaev, R., Wu, F., Anghel, A., Maruyama, N., Anderson, D. N., et al. (2008). Impact of terrestrial weather on the upper atmosphere. *Geophysical Research Letters*, *35*(9), L09808. https://doi.org/10.1029/2007GL032911

Fuller-Rowell, T. J., Fang, T.-W., Li, Z., Fedrizzi, M., Sutton, E. K., Iye, S., & Jah, M. (2022). *Neutral density from operational whole atmosphere models for satellite drag and space traffic management*. COSPAR 44th Scientific Assembly. Retrieved from https://ui.adsabs.harvard.edu/abs/2022cosp…44.853F/abstract

Huang, C., Huang, Y., Su, Y.-J., Sutton, E. K., Hairston, M. R., & Coley, W. R. (2016). Ionosphere-thermosphere (IT) response to solar wind forcing during magnetic storms. *Journal of Space Weather and Space Climate*, *6*, A4. https://doi.org/10.1051/swsc/2015041

Jackson, D. R., Bruinsma, S., Negrin, S., Stolle, C., Budd, C. J., Dominguez Gonzalez, R., et al. (2020). The space weather atmosphere models and indices (SWAMI) project: Overview and first results. *Journal of Space Weather and Space Climate*, *10*, 18. https://doi.org/10.1051/swsc/2020019

Maruyama, N., Sun, Y.-Y., Richards, P. G., Middlecoff, J., Fang, T.-W., Fuller-Rowell, T. J., et al. (2016). A new source of the midlatitude ionospheric peak density structure revealed by a new Ionosphere-Plasmasphere model. *Geophysical Research Letters*, *43*(6), 2429–2435. https://doi.org/10.1002/2015GL067312

Picone, J. M., Hedin, A. E., Drob, D. P., & Aikin, A. C. (2002). NRLMSISE-00 empirical model of the atmosphere: Statistical comparisons and scientific issues. *Journal of Geophysical Research*, *107*(A12), 1468. https://doi.org/10.1029/2002JA009430

Qian, L., Wang, W., Burns, A. G., Chamberlin, P. C., Coster, A., Zhang, S.-R., & Solomon, S. C. (2019). Solar flare and geomagnetic storm effects on the thermosphere and ionosphere during 6–11 September 2017. *Journal of Geophysical Research: Space Physics*, *124*(3), 2298–2311. https://doi.org/10.1029/2018JA026175

Richards, P. G. (2013). Reevaluation of thermosphere heating by auroral electrons. *Advances in Space Research*, *51*(4), 610–619. https://doi.org/10.1016/j.asr.2011.09.004

Richards, P. G., & Torr, D. G. (1996). The field line interhemispheric plasma model. In R. Schunk (Ed.), *Solar terrestrial energy program ionospheric model handbook* (pp. 207–216). Utah State University.

Tapley, B., Schutz, B. E., & Born, G. H. (Eds.). (2004). *Statistical orbit determination* (p. 547). Elsevier Academic Press. https://doi.org/10.2514/1.30038